

Designing Strength-Proportional Hydraulic Resistance for an Elbow Flexion-Extension Exercise Machine

Brian A. Garner

Department of Mechanical Engineering,
Baylor University,
Waco, TX 76798-7356

The mechanical linkage of a hydraulic-resistance, elbow flexion and extension exercise machine was redesigned to provide a resistance response that varies in proportion to female joint strength over the range of motion. The aim was to integrate into a simple, passive exercise machine the respective benefits of hydraulic resistance and isokinetic exercise. Hydraulic resistance facilitates bidirectional, concentric-concentric exercise that naturally scales to accommodate users of varying strength. Strength-proportional resistance emulates the response of isokinetic exercise to work muscles at their maximum capacity throughout the range of motion. Methods: Independent mathematical models of elbow joint strength and machine resistance were derived as a function of machine arm flexion angle and angular velocity. The strength model was based on experimental data measured from female subjects during maximum-effort trials on the exercise machine. The resistance model was based on the force-velocity response of the hydraulic cylinder and the linkage's mechanical advantage as determined from its geometric parameters. The intersection of these two models was assumed to represent conditions of equilibrium between strength and resistance, and was used to predict exercise operating speed for any angle of elbow flexion. Numerical optimization methods were applied to compute optimal parameters for two-bar and four-bar linkage configurations with the objective of achieving predicted operating speed patterns that were constant (isokinetic) over the range of motion. Results: A four-bar linkage configuration was found to be more effective at providing the desired resistance response than a two-bar configuration. Experimental trials using the optimized linkages confirmed model predictions and demonstrated that user operating speeds over the range of motion were closer to the desired isokinetic patterns than with the original linkage. The design method was effective at predicting user operating speeds and targeting desired shapes and magnitudes for the operating speed patterns. The method should be applicable to the design of other exercise machines that seek the advantages of a strength-proportional response derived from hydraulic resistance. [DOI: 10.1115/1.2355684]

Introduction

Various forms of exercise are well recognized for their benefits and limitations [1–4]. Isometric exercise, which is performed against an immovable resistance, is effective for isolating particular muscle groups and strengthening joints limited by pathology, injury, or bracing. However, strength improvements are limited to the joint position exercised, and fall off at positions away from this point [1–4].

Isotonic exercise works muscles over a range of joint positions against a generally constant resistance load. Examples include pull-ups and push-ups, and exercises involving free weights and certain types of weight-stack machines (e.g., select models by Paramount Fitness Corporation and Universal Gym Company). This and other forms of resistance exercise can improve muscle strength and endurance, preserve mean body mass, maintain metabolic rate, preserve bone mineral density and content, and contribute to weight reduction [1,5–7]. However, the constant resistance of isotonic exercise does not generally correspond to the varying strength capacity of joints over the range of motion. Therefore, the resistance load can be no greater than the joint strength at the weakest point, leading to submaximal effort for most of the range

of motion, and risking the “sticking” effect that is common in such exercises as the squat and bench press [8,9].

Isokinetic exercise [1–4,10] is characterized by a resistance load that varies dynamically over the range of motion to accommodate changes in joint strength and to maintain a prescribed, constant exercise velocity. Computer-controlled isokinetic exercise machines employ dynamometers, feedback, control, and actuation systems to safely increase or decrease resistance in response to user effort (e.g., Biodex Medical Systems, Inc., Cybex International, Inc.). Some have argued that isokinetic exercise training leads to optimal strength increases because muscles may work at their maximum capacity over the full range of joint motion [9,10]. It has proven effective for aerobic conditioning, muscle strengthening, and joint rehabilitation [2,10]. However, the complexity, bulk, and expense of these systems limit their use primarily to research and clinical settings.

Other, more accessible types of exercise machines seek to emulate the isokinetic response using *passive* resistance designed to vary in proportion with joint strength over the range of motion [4,11]. Common designs employ cams, cables, and weight stacks to provide variable resistance appropriate for a specific, single-degree-of-freedom exercise motion (e.g., Nautilus, Inc., Cybex International, Inc., Universal Gym Company). This form of exercise has proven effective for muscular gains, weight control, aerobic conditioning, and rehabilitation [4,6,12,13]. However, these types of machines provide only unidirectional, concentric-eccentric ex-

Manuscript received February 1, 2006; final manuscript received July 19, 2006. Review conducted by M. Y. Lee.



Fig. 1 Adjustable prototype configured like the original elbow flexion and extension exercise machine. The user sits with the upper arms resting against the elbow pads, and operates the machine arms in cyclic, reciprocal elbow flexion and extension motion as fast as possible against the hydraulic cylinder resistance.

ercise, they require manual adjustment of the weight stack for each user; and the actual correlation between the machine resistance and human strength capacity has been questioned [14–17] (see Discussion).

The aim of this study was to design an exercise machine that provides passive, strength-proportional variable resistance using hydraulics as the resistance mechanism. Hydraulic resistance can operate bidirectionally so that opposing muscle groups work concentrically with a lower risk of muscle soreness and injury than with eccentric exercise [1,4,10,18–20]. Also, the passive damping response of hydraulics naturally scales to accommodate users of varying strengths, obviating the need for a weight stack and permitting a simpler, less-bulky machine. However, the design of hydraulic-resistance exercise machines is complicated by the fact that the resistance load is derived from the *velocity* of the hydraulic cylinder piston rather than, for example, the *position* of a cam. The hypothesis motivating this study was that the mechanical linkage of a hydraulic-resistance exercise machine could be strategically designed to transmit velocity to the cylinder, and resistance to the user, to complement joint strength capacity and emulate isokinetic exercise over the range of exercise motion.

The object of this work was an elbow flexion and extension exercise machine (EFM) used as part of a women's fitness program. An adjustable prototype of the machine (Fig. 1) was constructed to facilitate the study and configured with the same geometry as the original. The machine provides bilateral resistance by way of two, independently moving arms, each attached to a separate hydraulic cylinder. Patrons are trained to operate the arms in reciprocal, cyclic strokes as fast as possible (i.e., maximum voluntary effort) through the range of motion. Because of the machine's symmetry, only the right-hand side was analyzed in this study.

This paper presents the methods and results of four sequential phases of the study followed by discussion and conclusions. In the first phase, the characteristic elbow flexion and extension strength

of women was measured using the prototype EFM. In the second phase, the generalized resistance response of the EFM was analyzed and modeled. In the third phase, the previous results were used to develop a modified linkage for the machine designed to emulate isokinetic exercise. In the final phase, the new linkage configuration was evaluated experimentally.

Measuring Characteristic Joint Strength

Methods. A series of experimental measurements were performed to characterize female elbow joint strength on the EFM prototype during maximal, voluntary flexion and extension exercises. Experiments in this study were performed with Baylor University IRB approval and the signed consent of participants. Six female volunteers with no reported history of injury to the right shoulder or arm were recruited from the Baylor community. Subjects ranged in age from 20 to 53 years, in height from 157 cm (62 inches) to 170 cm (67 inches), and in weight from 52 kg (115 lb) to 87 kg (192 lb). All subjects were regular participants in the women's fitness program, and were familiar with the EFM.

Motion and force data were collected during the experimental trials. A three-camera, video motion capture system (zFlo, Inc., Quincy, MA) was used to record motion of adhesive reflective markers affixed to the EFM base, its moving arm, and the subjects' right shoulder, elbow, and wrist. Force generated in the hydraulic cylinder was measured by a 500-lbf (2.24 kN) load cell (Transducer Techniques, Inc., Temecula, CA) mounted between the cylinder casing and its attachment point on the EFM base. To accommodate the small additional length imposed by insertion of the load cell, the cylinder attachment point was shifted downward on the base in a direction parallel to the piston rod (to minimize any affect on the cylinder's mechanical advantage).

The experimental protocol involved several minutes of light warm-up exercise followed by a series of maximal-effort trials. For each trial the subjects were asked to begin with the right arm flexed and the left arm extended, and commence exercise upon hearing the audible signal. Subjects were instructed to exercise both arms in reciprocal, cyclic flexion and extension throughout the range of motion as fast as possible for five complete cycles. Three levels of hydraulic resistance (light, normal, and heavy) were used for the trials to elucidate joint moments at various operating speeds (fast, normal, and slow, respectively). The original EFM hydraulic cylinder provided the normal resistance, and two custom-built cylinders provided the light and heavy resistance, respectively. Between each trial subjects were asked to rest for at least 90 s while the cylinders were exchanged in preparation for the next trial.

Load cell data was collected at 100 Hz and subsequently re-sampled at 60 Hz for alignment with the video data. The analog and video data were synchronized based on a visual cue (LED flash) generated by the analog transducer and recorded in the video. The flexion angle of the machine arm (corresponding to flexion of the elbow) was computed from the motion capture data for each video frame and differentiated to obtain angular velocities. Joint moments generated by the subjects against the machine arm were calculated as the product of the measured load-cell force and the computed mechanical advantage (MA) of the machine linkage (explained below) at the corresponding machine angle.

Data collected over the five cycles of each trial were reduced to a single pair of data sets representing one stroke of elbow flexion and one stroke of elbow extension. To achieve this reduction the trial data was sorted according to machine arm flexion angle and segregated into consecutive 10 deg windows over the range of motion. The peak flexion moment and the corresponding flexion angle and angular velocity within each window were extracted and collected to form the flexion stroke data for the trial. Similarly, the peak extension moment and the corresponding flexion angle and angular velocity within each window were extracted and collected to form the extension stroke data.

Regression models were developed to characterize the flexion

strength and extension strength of the subjects. The data from two subjects whose flexion and extension moments fell midrange within those of the other subjects were selected to be representative of the group. The flexion stroke data and the extension stroke data from the various trials of the two subjects were combined to represent the group's flexion strength and extension strength, respectively. A two-variable, second-order polynomial regression equation was fit to each collection of strength data ($R^2=0.87$ for flexion, 0.89 for extension) to form a three-dimensional surface model [21] characterizing maximum voluntary joint moment as a function of machine arm flexion angle, θ , and angular velocity, $\dot{\theta}$,

$$\begin{aligned}\tau_F &= \Phi_F(\theta, \dot{\theta}) \\ \tau_E &= \Phi_E(\theta, \dot{\theta})\end{aligned}\quad (1)$$

where τ is the joint strength moment, Φ is the second-order polynomial surface regression equation, and the subscripts refer to flexion (F) and extension (E), respectively. These regression models were derived from data somewhat scattered over the space of flexion angle and angular velocity, but they permit the calculation of approximate maximum joint moments at any reasonable state of joint angle and angular velocity. For comparison with other experimental strength data reported in the literature, the models were used to calculate equivalent *isokinetic* joint strengths for the subjects at various speeds over the range of motion.

Results. The maximal isokinetic joint moments calculated using the subject strength models over the range of motion compared well with the isokinetic strength data reported by Knapik [22] (Fig. 2). The flexion moments exhibit magnitudes and trends similar to the literature data, but appear shifted about 30 deg towards extension. The modeled peak flexion moments occur near 60 deg flexion compared with 90 deg flexion in the literature data. In addition, the modeled flexion moments fall off more rapidly than the literature data at high angles of flexion. The extension moments trend more closely with the literature data than the flexion moments. The modeled extension moments appear shifted about 10 deg towards extension, with peak extension moments occurring at 60 deg flexion for the modeled data and 70 deg for the literature data. As with flexion, the modeled extension moments again drop off more dramatically than the literature data at high flexion angles. For both flexion and extension the magnitude of the modeled peak moments at 108 deg/s are nearly equivalent to those of the literature data (~ 25 Nm flexion, ~ 28 Nm extension). For isokinetic speeds of 180 deg/s, the modeled peak moments (18 Nm flexion, 21 Nm extension) are slightly lower than the corresponding literature data (20 Nm flexion, 25 Nm extension). These observed discrepancies may stem from machine and postural differences between the specifically isokinetic literature studies and this study designed to measure strength during regular exercise. For example, on the EFM the gap between the two arm pads permits approximately 15 deg laxity between the user's forearm and the machine arm (see Fig. 1), and the user's shoulder and elbow are free to rotate and translate as elbow angle varies. For purposes of designing a resistance response for regular exercise, the subsequent analysis was based on the data collected in this study using the prototype exercise machine.

Modeling the Resistance Response

Methods. The resistance moment of the EFM against the user's arm was modeled as the product of hydraulic cylinder force and mechanical advantage

$$T = F(v) \cdot MA(\theta) \quad (2)$$

where T is the resistance moment (torque) about the machine arm axis, F is the force-velocity response of the hydraulic cylinder, v is the cylinder piston velocity with respect to the cylinder casing, MA is the mechanical advantage (defined below) of the machine

Maximum Voluntary Flexion Moment (Nm)

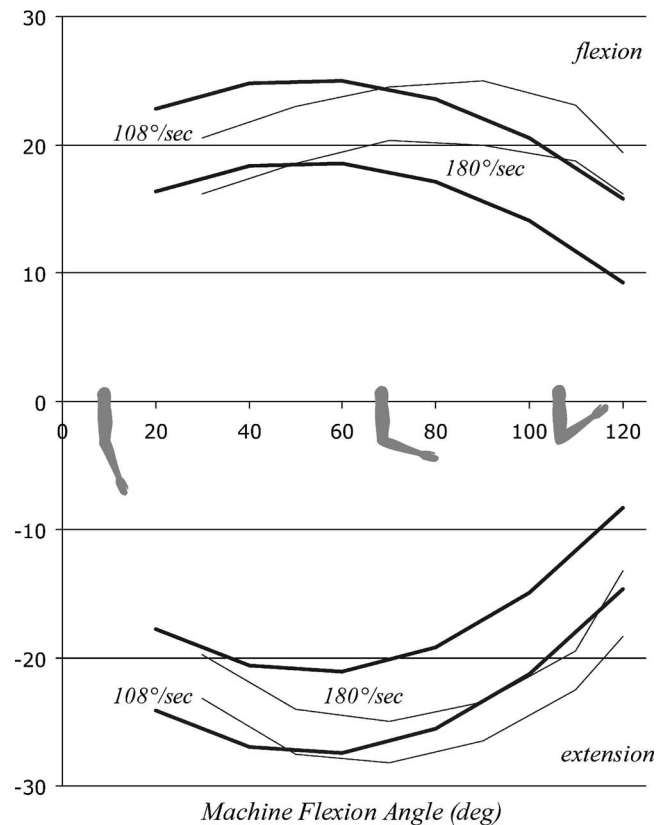


Fig. 2 Female maximum voluntary elbow flexion and extension moments at isokinetic speeds of 108 deg/s and 180 deg/s over a range of elbow joint angles. Data collected on the prototype exercise machine of this study (thick lines) compares well with data (thin lines) reported by Knapik [14].

linkage, and θ is the machine arm flexion angle.

The force-velocity response of the hydraulic cylinder was measured using an MTS 858 Mini Bionix II mechanical testing system (MTS Corporation, Eden Prairie, MN) programmed to drive the piston through cyclic tension and compression strokes at various constant velocities (i.e., a sawtooth displacement profile). The force induced in the cylinder was sampled at 100 Hz, and an average force value was computed for each velocity in tension and compression, respectively. The force response was found to be independent of piston displacement, and to be slightly greater in tension than in compression (Fig. 3). A second-order polynomial regression equation was fitted ($R^2 > 0.99$) to each set of these data

$$F_T = \Pi_T(v) \quad (3)$$

$$F_C = \Pi_C(v)$$

where Π is the regression equation, and the subscripts correspond to tension (T) and compression (C), respectively.

The mechanical advantage (MA) of the machine linkage was defined as the partial derivative of cylinder piston displacement, ℓ , with respect to the flexion angle, θ , of the machine arm

$$MA = \frac{\partial \ell}{\partial \theta}(\theta) \quad (4)$$

where the partial derivative was derived from the machine's linkage geometry (see Appendix). The MA has units of length representing the leverage transmitting cylinder force into resistance moment at the machine arm, and its value varies as a function of θ over the range of exercise motion (Fig. 4). For the simple two-

Cylinder Force (N)

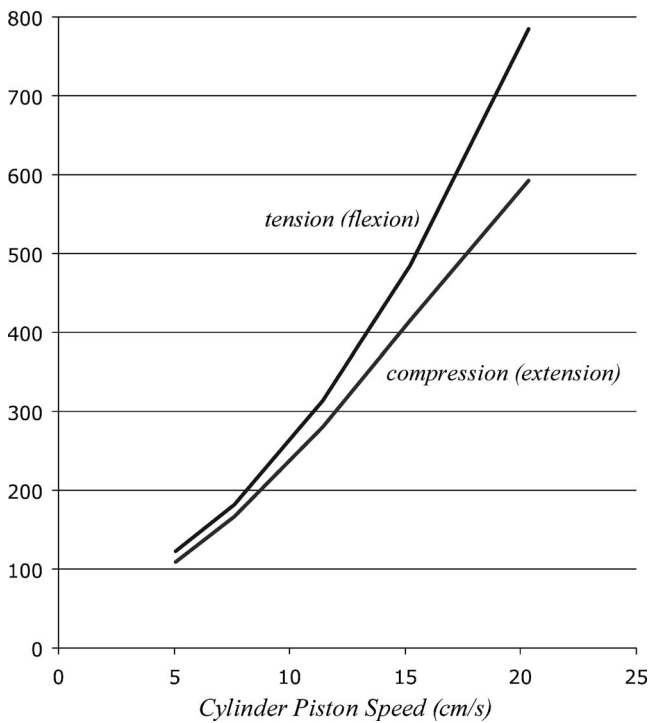


Fig. 3 Measured force-velocity response of the hydraulic cylinder that provides resistance for the elbow flexion and extension exercise machine. Resistance naturally increases with piston speed, and was found to be slightly higher when the cylinder was loaded in tension (corresponding to elbow flexion) than in compression (corresponding to elbow extension).

Mechanical Advantage (cm)

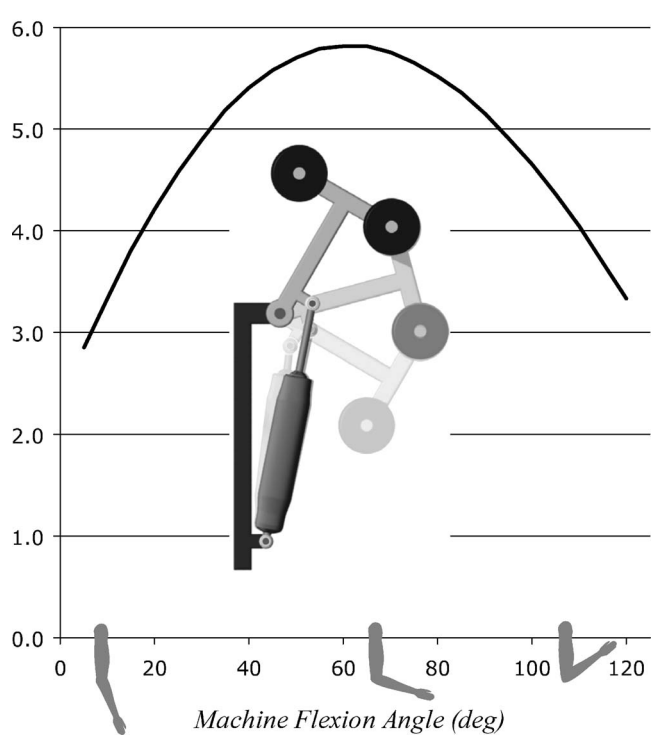


Fig. 4 Mechanical advantage (leverage) transmitting hydraulic cylinder force into resistance moment at the machine arm (inset). The higher mechanical advantage in the middle of the range of motion provides increased resistance where the elbow joint is strongest.

bar geometry of the original EFM configuration (Fig. 4, inset), the MA is identical to the perpendicular distance between the hinge axis and the cylinder piston rod. An expression for the cylinder piston velocity follows from Eq. (4) as

$$v = MA(\theta) \cdot \dot{\theta} \quad (5)$$

where $\dot{\theta}$ is expressed in radians. Finally, Eqs. (2)–(5) can be combined to construct a three-dimensional surface model representing the generalized resistance moment of the machine as a function of both machine arm flexion angle and angular velocity,

$$T_F = \Pi_T(MA(\theta) \cdot \dot{\theta}) \cdot MA(\theta) \quad (6)$$

$$T_E = \Pi_C(MA(\theta) \cdot \dot{\theta}) \cdot MA(\theta)$$

where machine arm flexion is associated with tension in the cylinder piston rod, and extension is associated with compression.

The surface models expressed by Eqs. (1) and (6) represent the capacity of the user to generate moment (strength), and the capacity of the machine to resist moment (resistance), respectively, for varying states of machine arm flexion angle and angular velocity (Fig. 5). The relationship between these surface models was used to predict the speed at which a user would operate the machine arm during maximal-effort exercise. Since strength naturally decreases with speed (Fig. 5, strength surface), and resistance naturally increases with speed (Fig. 5, resistance surface), it follows that at any given moment during exercise motion the user will drive the machine arm at a speed where the strength moment is counterbalanced by the resistance moment (neglecting inertial influences; see Discussion). This condition of equalized strength and resistance was assumed to occur along the line of intersection between the strength and resistance surface models (Fig. 5, inter-

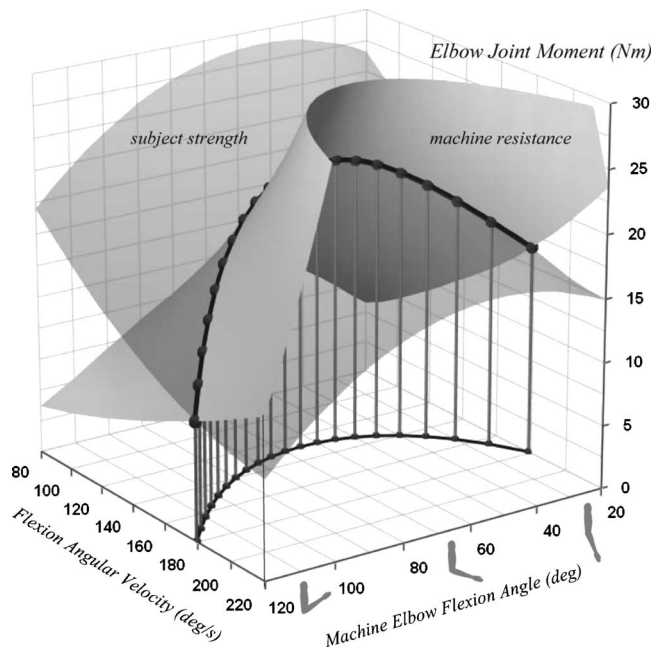


Fig. 5 Three-dimensional surface models representing female elbow flexion strength and machine arm flexion resistance, respectively, as a function of machine flexion angle and angular velocity. Exercise is assumed to occur over the range of motion at speeds where strength is equalized by resistance (line of intersection between surfaces, and its projection).

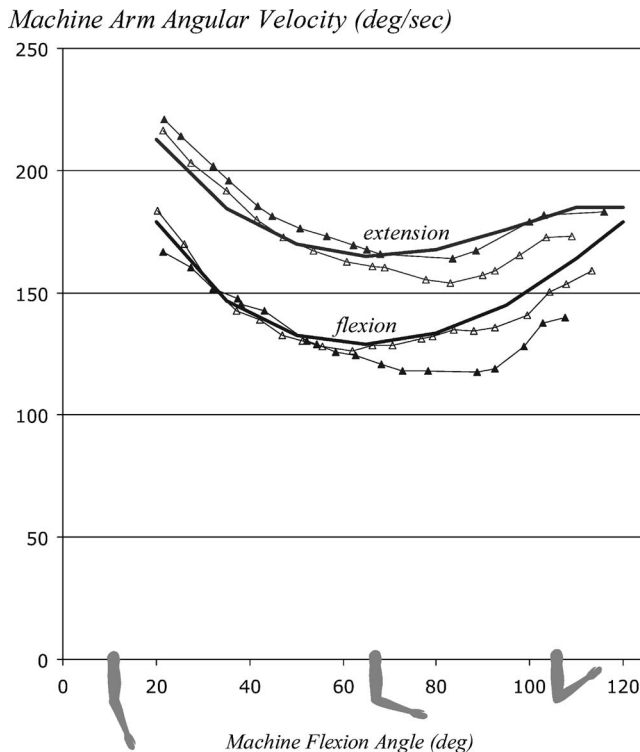


Fig. 6 Predicted (thick lines) and observed (thin lines) user operating speeds for maximal-effort elbow flexion and extension exercise over the range of motion. The predicted values compare well with the observed data from two representative subjects (filled and unfilled triangles, respectively).

section line). Points on this line of intersection at discrete machine flexion angles were computed using an iterative, root-solving approach, and the corresponding angular velocities (Fig. 5, projected intersection line) were compared with the actual operating speeds observed during the experimental trials.

Results. The predicted operating speeds exhibited a parabolic pattern with higher speeds near full extension and full flexion, and the lowest speeds near midrange (for flexion, see Fig. 5, projected intersection line). This pattern was predicted for both flexion and extension, and agreed well with the operating speeds observed for the two representative subjects (Fig. 6). For flexion, the predicted and observed data are nearly identical over the range of angles from full extension to about 65° flexion. For the remaining range of flexion angles, speeds for the two subjects begin to diverge from each other and trend somewhat below the predicted values. The predicted flexion speeds range from 129 deg/s at the lowest point near 65 deg elbow flexion, to 180 deg/s at both extremes of the range of motion (a 40% increase). For extension, the predicted and observed data also track closely over the range of angles from full extension to about 70 deg flexion, though the subject speeds are slightly higher. Over the higher angles of flexion, the experimental data again diverge and trend below the predicted values, but both the predicted and observed data remain relatively low compared to speeds near full extension. The predicted extension speeds range from 165 deg/s at the lowest point near 65 deg elbow flexion to 212 deg/s at full extension (a 29% increase). At 120 deg flexion the predicted extension speed rises to 185 deg/s, 12% above the lowest point.

Designing a Modified Linkage

Methods. To achieve more constant exercise operating speeds over the range of motion, the mechanical linkage between the hydraulic cylinder and the machine's user-driven arm was modi-

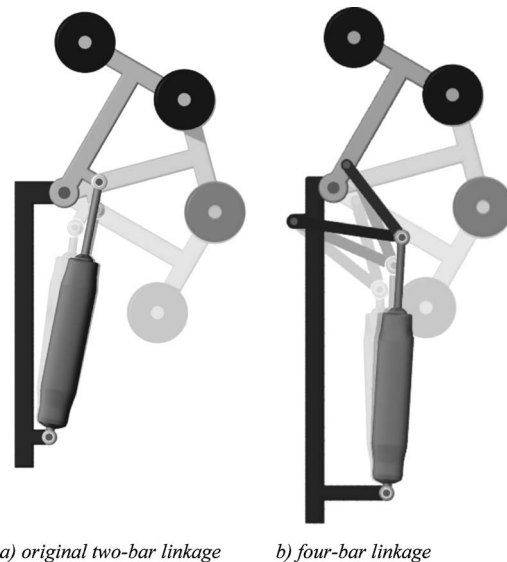


Fig. 7 Linkage configurations of (a) the original two-bar design and (b) the modified four-bar design. In both cases the cylinder piston rod is displaced by user actuation of the padded machine arm.

fied. The modifications were designed to alter the machine's MA, and thus its resistance response (Eq. (6)), so as to effect operating-speed patterns more closely resembling isokinetic exercise. Both two-bar and four-bar linkage designs were considered (Fig. 7). As with the original two-bar linkage, the MA of the four-bar linkage was defined by Eq. (4) and computed according to its geometry (see Appendix) as a function of machine arm flexion angle.

Parameters describing the geometry of each linkage configuration (see Appendix, Fig. 11) were optimized using an iterative, numerical approach. Theoretically, any desired resistance response could be targeted using this approach by specifying an appropriate optimization objective function. The optimization objective function used in this study was selected to minimize the deviation between predicted maximal-effort operating speeds and those of purely isokinetic exercise. The steps of the optimization approach included the following:

- (1) Assign reasonable initial values to all linkage parameters.
- (2) Reconstruct the resistance surface model via Eqs. (4)–(6).
- (3) Compute the intersection between strength and resistance surface models.
- (4) Evaluate the objective function based on predicted speeds at the intersection.
- (5) Adjust linkage parameters to improve objective function performance.
- (6) Iterate from step (2) until no further improvement is needed.

A simple, steepest-descent optimization algorithm, with occasional random perturbations to avoid local minima, was used in step (5) to guide adjustments of the linkage parameters. The optimization objective function was specifically defined to minimize the error between the predicted operating speeds and selected target isokinetic operating speeds, accumulated over the range of motion for both flexion and extension

$$f = k_{\text{ext}} \sum_i^n |\dot{\theta}_i - \dot{\theta}_*|_{\text{extension}} + k_{\text{flx}} \sum_i^n |\dot{\theta}_i - \dot{\theta}_*|_{\text{flexion}} \quad (7)$$

where f is the performance measure, $\dot{\theta}_i$ is the predicted angular velocity at machine arm flexion angle i over the selected range of n discrete angles, and $\dot{\theta}_*$ is the constant target angular velocity, for

Table 1 Values of targeted isokinetic exercise speeds ($\dot{\theta}$) used in Eq. (7) for computation of optimal machine linkage geometries. Three optimal linkage geometries were computed to effect desired slow, moderate, and fast exercise speeds, respectively. Because experimental measurements indicated that elbow extension was stronger than elbow flexion, faster operating speeds were targeted for extension than for flexion in each case.

	Flexion $\dot{\theta}_*$ (deg/s)	Extension $\dot{\theta}_*$ (deg/s)
Slow	90	110
Moderate	135	163
Fast	180	215

extension and flexion as indicated. The weighting coefficients k_{ext} and k_{flx} were each assigned a value of one to optimize equally for both extension (k_{ext}) and flexion (k_{flx}).

Three optimal linkage solutions were computed using various values of $\dot{\theta}_*$ to achieve desired slow, moderate, and fast isokinetic exercise speeds. For each solution different target speeds were chosen for flexion and extension, respectively (see Table 1), based on the operating speeds observed during the experimental measurements. All solutions assumed that the machine was equipped with the original hydraulic cylinder providing a normal level of resistance. Two ancillary linkage solutions were also computed for each of the three desired exercise speeds: one using only the extension component of error in Eq. (7) ($k_{ext}=1, k_{flx}=0$), and the other using only the flexion component of error ($k_{ext}=0, k_{flx}=1$). The ancillary solutions permitted comparison between linkages optimized for flexion only, for extension only, and for both flexion and extension.

Results. The optimized solutions revealed that no amount of variation to the two-bar linkage configuration could produce appreciable improvement in the predicted operating speeds according to the objective function of Eq. (7). However, optimization of the four-bar linkage configuration did result in improved operating speed patterns. Figure 8 shows the MA curves of the optimized four-bar linkages compared with that of the original two-bar linkage. The four-bar MA curves exhibit the same inverted-parabola pattern as that of the two-bar MA curve, but the four-bar curves fall off less severely, maintaining greater resistance where needed at either end of the range of motion. For each four-bar linkage the peak MA occurs near 60 deg flexion angle, which is near that of the original two-bar linkage, and which corresponds to the flexion angle of peak experimental joint moments (see Fig. 2, thick lines). As expected, MA values are larger for linkages designed for slower operating speeds where more resistance is needed, and smaller for linkages designed for faster operating speeds where less resistance is needed. Finally, the MA curves of the primary and ancillary linkage solutions are quite similar for each target exercise speed (slow, moderate, and fast). This result reflects the symmetry in shape between the flexion strength curves and extension strength curves (Fig. 2), and suggests that a single linkage design may be sufficient to serve both exercise directions well (see Discussion).

Evaluating the Modified Linkage

Methods. A series of experiments was performed to evaluate the performance of the three primary four-bar linkage solutions. As much as possible these experiments were designed to follow the procedures used in the first series of experiments by which subject strength was characterized. Six female subjects participated in the experiments, most having also participated in the strength experiments. The prototype machine was refitted on the right- and left-hand sides with adjustable four-bar linkages that could be set to the parameters of any one of the optimized linkage

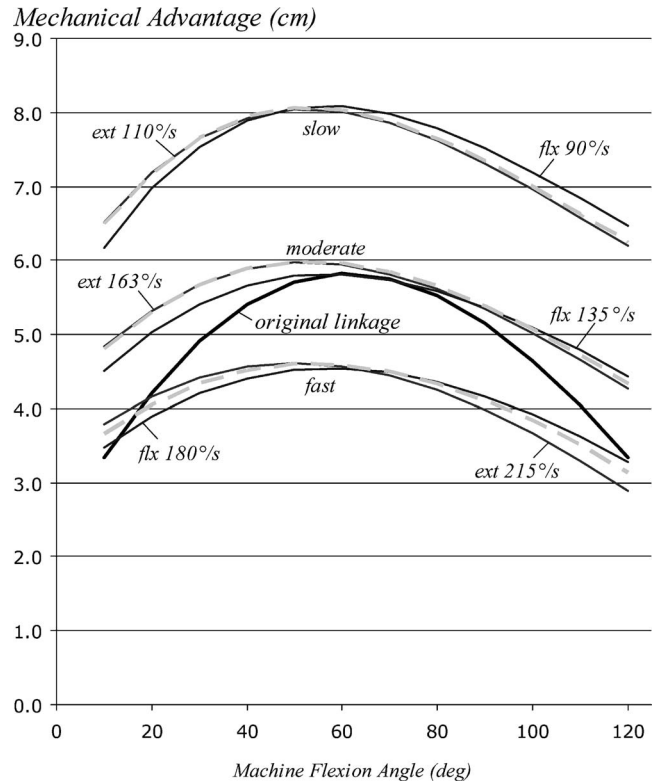


Fig. 8 Mechanical advantage as a function of machine arm flexion angle for the original two-bar linkage (thick solid line) and the optimized four-bar linkages (thin and dashed lines). Four-bar linkage designs were optimized to effect fast, moderate, and slow target operating speeds, and to prioritize only the extension stroke (ext, thin lines), only the flexion stroke (flx, thin lines), or both strokes equally (dashed lines). See text and Table 1 for details.

solutions. The original hydraulic cylinders, providing a normal level of resistance, were used for all trials. The motion capture system, adhesive markers, and load cell were employed as before.

The experimental protocol involved several minutes of light warm-up exercise followed by a series of three maximal-effort trials—one for each optimized linkage solution. For each trial subjects were asked to complete five flexion-extension cycles over the range of motion as quickly as possible. Between trials subjects were given several minutes to rest their arms while the four-bar linkages were adjusted to the parameters of the next trial. For half of the subjects the trials were scheduled in an order using the optimized fast, moderate, and slow linkage parameters, respectively. For the remaining subjects the order of trials was reversed. Data were collected and reduced in a manner similar to that used in the previous series of experiments.

Results. The magnitudes and trends of the measured operating speeds compared well with the predicted values for all three optimized four-bar-linkage solutions. Figure 9 shows the target, predicted, and average-of-measured operating speeds over the range of motion. As expected, the predicted operating speeds were relatively constant over the range of motion, and centered well on the respective target speeds. Similarly, the measured operating speeds, particularly that for flexion, were relatively constant over the range of motion. The measured speeds for extension were fairly linear over the range of motion, but exhibited a slightly negative slope that deviated from the desired constant target speeds. Measured speeds using the slow and moderate linkage designs tended to be somewhat slower than predicted, and measured speeds using the fast linkage design tended to be somewhat faster than pre-

Machine Arm Angular Velocity (deg/sec)

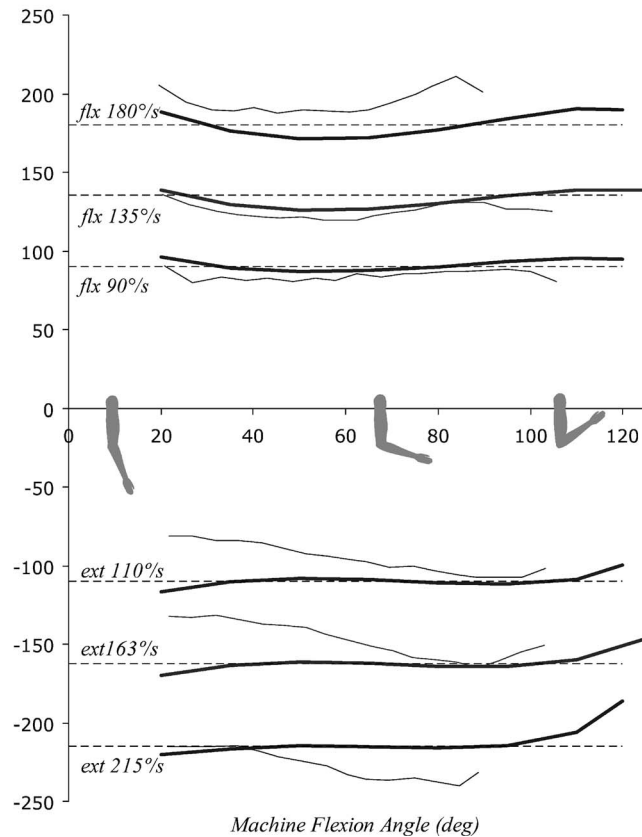


Fig. 9 Target (dashed lines), predicted (thick lines), and observed (thin lines) exercise operating speeds for the three four-bar linkage solutions optimized to prioritize both the flexion stroke (flx) and extension stroke (ext) equally. The observed operating speed data represents the average over all subjects.

dicted. Measured flexion speeds for the slow and moderate linkage designs were nearly identical to the predicted values over the range of motion.

Compared with the observed operating speeds using the original two-bar design, those of the four-bar designs tended to be more constant over the range of motion. Figure 10 shows the range and average of subject operating speeds for the original two-bar linkage and the optimized, moderate-speed four-bar linkage. For elbow flexion, a significant decrease in the change of operating speed over the range of motion is achieved by modifying the linkage. The average two-bar flexion speed varies 50 deg/s over the range of motion from its minimum of 137 deg/s near mid-range to 187 deg/s near full extension (a 36% increase). The average four-bar speed varies only 17 deg/s from its minimum of 119 deg/s near mid-range to 136 deg/s near full extension (a 14% increase). For elbow extension, the decrease in the change of operating speed over the range of motion is less than that for flexion, but is still significant. The average two-bar extension speed varies 60 deg/s (from 164 to 224 deg/s, a 36% increase) compared with the average four-bar extension speed, which varies 33 deg/s (from 132 to 165 deg/s, a 25% increase). The four-bar operating speeds for both flexion and extension exhibited a shallow sinusoidal pattern compared with the rather pronounced parabolic shape of the two-bar operating speeds. This predicted feature (see Fig. 9), despite the slight negative slope in the extension speeds, further served to maintain a relatively constant operating speed over the range of motion. Finally, Fig. 10 reveals that the distribution of operating speeds among subjects using the four-bar linkage is narrower than that of the two-bar

Machine Arm Angular Velocity (deg/s)

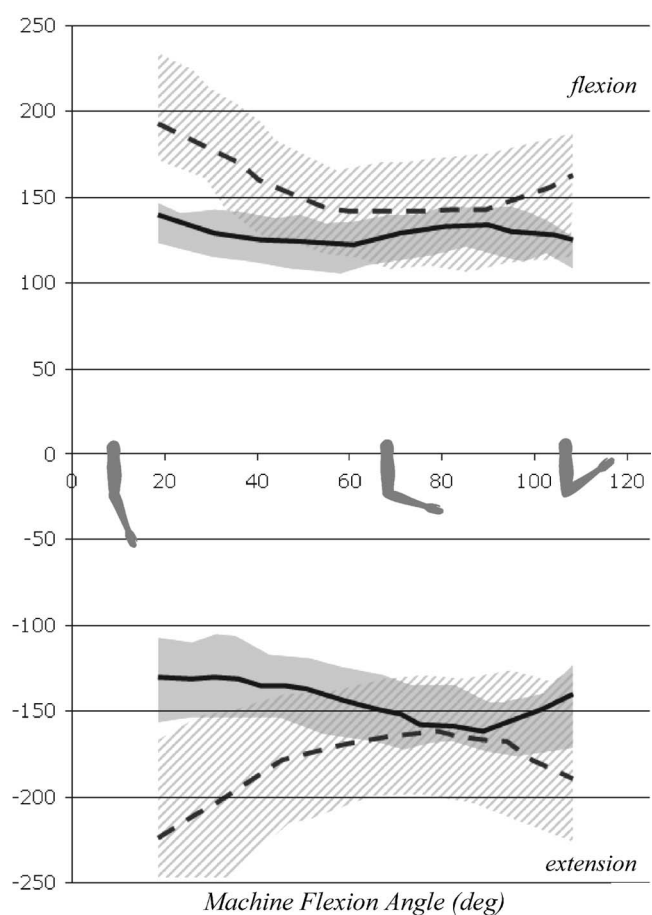


Fig. 10 The average (lines) and ranges of observed user operating speeds over all subjects for maximal-effort elbow flexion and extension exercise using the original two-bar linkage (dashed line and hatched region) and the moderate-speed four-bar linkage (solid line and shaded region). With the four-bar linkage the range of operating speeds is narrower across subjects, and is more constant over the range of motion.

linkage, perhaps due to the increased and more uniform resistance of the four-bar linkage over the range of motion.

Discussion

Background and Significance. Previous efforts to provide strength-proportional, variable resistance in exercise machines have most commonly used a combination of cams, cables, and weight stacks. Nautilus, Cybex International, Universal Gym Company, and others have lines of products based on this design concept. The cam in these machines serves to create a mechanical advantage between the user's joint moment and the constant gravitational force of the weights. Ideally, the shape of the cam may be designed to effect a resistance response that compliments user strength as a function of joint position over the range of motion. Some studies, however, have found that for a number of these machines measured resistance does not, in fact, correlate well with user strength [14–17]. One possible explanation for this discrepancy is that the resistance response of the weights does not depend solely on the position of the cam. For example, during the initiation of the stroke the user must overcome both the weight's force of gravity and the force required to accelerate the weight into motion. At the end of the stroke the weight's force of gravity is offset by its deceleration to a stop. Thus, inertial effects of the moving weights contribute to the resistance response as a function

of joint *acceleration*, which can be difficult to predict and may vary significantly between users.

Less common efforts to provide strength-proportional, variable-resistance in exercise machines have used elastic members as the resistance mechanism. Bokelberg and Gilmore [23] designed a passive elbow flexion machine using springs connected to a four-bar linkage, where the human arm served as one of the links. The geometric parameters of the linkage were optimized numerically to provide a theoretical resistance response that correlated with experimental strength data as a function of joint position. In their theoretical analysis, linear springs were found to be more effective than torsional springs for achieving the desired resistance response, but the effectiveness of the machine design was not verified experimentally. Like weights, elastic members are limited to unidirectional, concentric-eccentric forms of exercise.

A significant feature of this study is its aim of designing for strength-proportional, variable resistance exercise using hydraulic cylinders as the resistance mechanism. Unlike weights or springs, hydraulics (or other friction-based components) develop force as a function of velocity. Therefore, in combination with a position-dependent mechanical linkage, the overall resistance response of a hydraulic exercise machine must be designed as a function of both position and velocity. For example, the position dependence may be designed to be strength-proportional over the range of motion, and the velocity dependence may be designed to effect a desired magnitude for the operating speed. The appearance of both θ and $\dot{\theta}$ in Eq. (6) clearly shows that the position and velocity components of the resistance response are coupled so that both must be considered together in the design process. Note also in Eq. (6) that the linkage's MA appears twice, once in transmission of velocity to the cylinder, and again in transmission of resistance back to the user. In simple terms, for a given cylinder force-velocity response, the linkage must be designed to transmit the appropriate combination of velocity to the cylinder, and resistance moment to the user, for all positions over the range of motion.

One advantage of using hydraulic cylinders rather than weights and springs is that, because of the velocity dependence, the resistance scales naturally for users of varying strengths. That is, because the hydraulic resistance increases with velocity, a stronger user will naturally receive a higher resistance by operating the exercise machine at higher speeds. In addition, two factors combine to ensure that the difference between the higher speeds of stronger users and the lower speeds of weaker users remains narrow. First, the capacity of muscles to produce force naturally decreases with increased shortening velocity so that strength drops off with higher speeds. Second, the natural response of a simple hydraulic cylinder increases quadratically with velocity, resulting in resistance that increases steeply with higher speeds. Thus, with a relatively minor increase in operating speed, a significant increase in resistance relative to strength can be obtained. The result is that an appropriate resistance force should be achievable for all users without the need for manual adjustment of the number of weights or springs. And, the machine resistance can be designed to target a specific, narrow range of operating speeds for all users without significantly altering the position-dependent response over the range of exercise motion.

A second advantage of using hydraulic cylinders rather than weights and springs is that hydraulic cylinders operate bidirectionally. As a result, agonist and antagonist muscle groups can be exercised together on the same machine, and both muscle groups can be worked concentrically (during contraction) rather than eccentrically (during extension). While some studies show that eccentric exercise can be more effective at developing eccentric strength, it is also more likely to result in muscle soreness and structural damage to the muscle fibers [1,3,4,19,20]. The bidirectionality of hydraulic cylinders does, however, complicate the exercise machine design because the strength characteristics of the opposing muscle groups may not be symmetric over the range of

motion. Since the resistance response in each direction uses the same cylinder and linkage, the machine must be designed to accommodate the strength characteristics of both muscle groups simultaneously.

Few previous studies have used friction-based mechanisms specifically to provide variable resistance to match human joint strength. Petrosenko [24] developed an ankle exercising machine that used a slip-clutch and two independent cams to match plantarflexion and dorsiflexion strength, respectively. The resistance was controlled electronically, and involved a rather complex, bulky, and expensive system. Horowitz [25] developed a computer-controlled system which identified user strength in real time, and enforced a velocity profile optimized to elicit maximum instantaneous power from the user throughout the exercise motion. The device used a spring and four dynamically-adjustable dampers to provide resistance, though a compromise version used only a single passive damper. The method presented in this paper is designed to accomplish friction-based, strength-proportional, variable resistance without the complexity of a computer-controlled feedback system.

Features of Modeling Approach. The design approach used in this study relies upon three-dimensional surface models representing user strength [21] and machine resistance, respectively, as a function of joint position and velocity. The models were used to predict user operating speeds based on the assumption that the intersection of the surface models represents points of equilibrium between strength and resistance. While the user strength surface remains constant during the design process, the resistance surface changes with modifications to the linkage geometry. In this way the linkage may be designed so that the intersection occurs at the desired operating speed at each point over the range of motion. This approach inherently accounts for both the position-dependent (shape) and velocity-dependent (magnitude) components of the desired resistance response. It does not, however, directly account for the influence of inertia and gravity on the resistance response.

The effects of inertia on the machine's resistance response were assumed negligible compared to the resistance generated by the hydraulic cylinder. Inertial effects would only be significant if there were significant mass in the system and significant changes in velocity over the range of motion. Lacking a weight stack, the moving parts of the exercise machine contain relatively little mass. And, the resistance response was designed to effect *constant* operating speeds over the range of motion, with significant accelerations occurring only during transition phases when switching exercise directions. The experimental data support the assumption that inertial effects were not a significant component of resistance. Subjects were able reverse directions with angular accelerations exceeding 5000 deg/s², while angular accelerations during the stroke in each direction were generally less than 300 deg/s².

The effects of gravity were also neglected as a literal component of resistance in the modeling approach. That is, gravitational forces were not included in the equations of equilibrium between strength and resistance. However, because gravity was acting on the subjects during the experimental trials, gravitational effects were included in the data from which the strength model was derived. Thus, because the orientation of the user and machine with respect to gravity was not modified, these effects were implicitly included in the design process. And, if needed, the modeling approach could easily be adapted to account for gravity directly by adding its effect as a component to the resistance surface as a function of position.

Any design approach seeking to provide strength-proportional exercise resistance must account for the strength characteristics of the exercise. In this study, a model for strength was derived from data measured using the actual exercise machine rather than from similar data available in the literature. As shown in Fig. 2, the collected data was very similar to the literature data, but some differences were apparent (e.g., the shifting of the flexion data). Use of data collected on the actual machine accounted for any

differences that may occur between the normal conditions of exercise and the carefully controlled conditions of typical literature studies. For example, subjects in this study were free to move their shoulders and elbows as they normally would during exercise. And, the contribution of gravity was not factored out in this study as it rightfully is in data reported in the literature.

Effectiveness of Modeling and Design Methods. The modeling approach proved reasonably successful at predicting the operating speeds of both flexion and extension on the EFM. For the original two-bar configuration, both the shapes and magnitudes of the predicted operating speeds were very similar to those of the measured operating speeds over the range of motion (see Fig. 6). This is perhaps not too surprising as the predicted values were derived from strength data obtained from the same experiments as were the measured operating speeds. However, the close agreement lends credence to the models of strength and resistance, and to the assumption that the intersection line reflects operating conditions. The minor differences between the predicted and measured operating speeds for the original two-bar configuration are likely due to the simplified polynomial strength model based on the combined data of two subjects. For the modified four-bar configuration, the shapes and magnitudes of the predicted operating speeds were also quite similar to the measured values over the range of motion (Fig. 9), though the predicted extension speeds did not match as closely as the predicted flexion speeds (discussed below). For both directions, however, the measured operating speeds exhibited the same shallow sinusoidal shape predicted by the model (Fig. 9, compare thick and thin solid lines).

The design method of this study was also effective at facilitating an improvement in the EFM linkage towards a more isokinetic resistance response over the range of exercise motion. The operating speeds measured on the original two-bar configuration suggested that resistance was too low compared to strength at low and high angles of flexion (Fig. 10, see higher operating speeds at these angles compared to mid-range angles for dashed lines and hatched regions). Initial efforts to improve the two-bar linkage revealed that it did not provide the flexibility required to maintain a sufficient MA over the wide range of motion (Fig. 8, see optimal four-bar MA's compared with two-bar MA). However, the four-bar linkage provided much more flexibility, and the optimized solutions resulted in measured operating speeds that remained much more constant over the range of motion, particularly for flexion (Fig. 10, see solid lines and grey regions). Interestingly, the four-bar linkage was so flexible that the predicted operating speeds were quite insensitive to some parameters, and so these parameters were assigned values based on secondary design criteria such as compactness and convenience of link attachment sites. The slight negative slopes in the measured extension speeds (Fig. 9, compare measured with predicted extension data) were not predicted by the modeling approach, and indicate that resistance became increasingly greater compared to strength as the arm moved into extension, resulting in gradually slowing operating speeds. The prediction errors may be due to inaccuracies in the extension strength data resulting from the high extension speeds in the original series of experiments (Figs. 6 and 10, extension data for two-bar linkage). Alternatively, they may be due to the fact that, as the experimental data showed, subjects did not translate their shoulders and elbows as much using the four-bar linkage as when using the two-bar linkage. This modification of technique may have altered the user's strength characteristics and distorted the model predictions. Nevertheless, the extension speeds using the four-bar linkage are closer to linear over the range of motion than when using the original two-bar linkage (Fig. 10). And, subjects using the four-bar linkage spoke qualitatively of a sense of improved uniformity in the resistance response.

The design method of this study proved effective for achieving the operating speed magnitudes targeted in each of the three optimized linkage solutions. Studies have shown that setting an appropriate level of resistance is important for optimizing exercise

objectives, which could be aerobic, strength, power output, or power efficiency [26,27]. The presented design method could be used to target any reasonable operating speed magnitude. Fast, moderate, and slow operating speeds were targeted by the respective optimized solutions, and for each, the predicted operating speeds were nearly identical to the target speeds for most all of the range of motion. In addition, the measured operating speeds exhibited magnitudes very close to the target speeds, though the measured speeds for the fast design were slightly faster, compared with the respective target speeds, than those of the moderate and slow designs. This discrepancy may reflect, again, that the experimental strength data at high speeds was less accurate than at the lower speeds.

Finally, the design method was successful at designing a resistance response appropriate for both flexion and extension of the elbow. Fortunately, the strength characteristics of flexion are fairly symmetric with the strength characteristics of extension (Fig. 2). Both exhibit a peak near the middle of the range of motion, and fall off towards either end. However, the magnitude of extension strength is slightly greater than that of flexion. And, considering that for this study the hydraulic cylinder force response is lower for compression (extension) than for tension (flexion) (Fig. 3), it is natural that operating speeds in extension were overall higher than those for flexion. To account for this difference in the design process, target speeds for extension were chosen (based on the experimental data) to be higher than those for flexion. As shown in Fig. 8, when linkage solutions were optimized for extension only, or for flexion only, the computed optimum MA's were quite similar for each respective desired speed (fast, moderate, or slow). Thus, it was possible to design a common linkage whose MA was reasonably appropriate for both flexion and extension, and whose resistance response resulted in generally isokinetic exercise patterns in each direction.

Conclusion

The work presented in this paper shows how strength-proportional, variable resistance using passive hydraulic cylinders can be achieved for a bidirectional, concentric-concentric elbow flexion and extension exercise machine. The design method using models of user strength and machine resistance was effective at predicting user operating speeds and facilitating linkage designs to prescribe target operating speed patterns. Patterns of constant operating speed over the range of motion were targeted for the purpose of emulating isokinetic exercise and providing strength-proportional resistance over the range of motion. This choice of operating speed pattern was arbitrary, however, and the method could be applied similarly to target other desired operating speed patterns. In addition, the method could be applied to design for other exercises or other exercise machines. Key considerations in such designs would include the type of linkage configuration and the characteristics of user strength. In this study a four-bar linkage was found to be effective for providing the moment-arm curves needed to create strength-proportional resistance. On other machines that do not have so wide a range of motion, or whose exercise strength patterns vary to a greater degree over the range of motion, a two-bar linkage or other simple mechanism may suffice. In addition, in this study the shape of the strength curves of the opposing muscle groups happened to be rather symmetric over the range of motion, which may not be the case for other exercises or other exercise machines. Asymmetric strength curves may make it impossible to design a common linkage that will precisely achieve desired operating speed patterns for both exercise directions, and so some compromise may be required. In such cases hydraulic cylinders that are valved to provide different levels of resistance in each direction may prove useful. Finally, the design approach of this study depends on an accurate model to represent user strength as a function of positions and velocities. The accuracy of model predictions of user operating speeds may have been improved in this study if a more complex strength

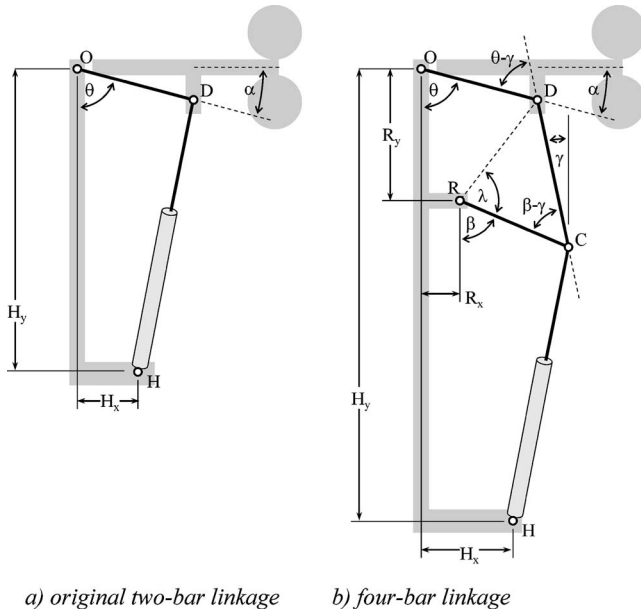


Fig. 11 Geometric parameters and other variables for describing the two-bar and four-bar linkages, and for deriving values of the mechanical advantage of each, respectively (see Appendix). Geometric parameters varied in order to optimize (see text) the respective mechanical advantages include: d (the length of link OD), α , H_x , and H_y in both linkages, and R_x , R_y , and c and r (the lengths of links DC and CR , respectively) in the four-bar linkage. Note that in Fig. 7(b) the optimized four-bar linkage is shown with parameter α set to zero.

model had been used, or if more dense and wide-ranging data had been available from which to derive the strength model.

Acknowledgment

Funding and support from Curves, International is greatly appreciated. Invaluable assistance from Baylor Engineering faculty, staff, and students, including Dr. Walter Bradley, Dr. Ian Gravano, Dr. Carolyn Skurla, Ashley Orr, Lauren Fincher, Marilyn Medlock, Blake Branson, and Brett Levins, is also gratefully acknowledged.

Appendix

The resistance moment of the exercise machine arm was computed as the product of the hydraulic cylinder force and the mechanical advantage (MA) of the linkage coupling the arm to the cylinder. For both the two-bar and four-bar linkage configurations, the MA was derived from geometrical parameters as shown in Fig. 11 and detailed below.

Two-Bar Linkage MA

The moment arm is defined as the partial derivative of the cylinder length with respect to the machine joint angle

$$MA = \partial \ell / \partial \theta$$

Segment lengths between points are defined as

$$d \equiv \overline{OD} \quad \ell \equiv \overline{HD}$$

where the cylinder displacement length ℓ can be computed between its attachment points H and D , and differentiated with respect to θ to give the MA,

$$\ell = \sqrt{(H_x - d \sin \theta)^2 + (H_y - d \cos \theta)^2}$$

$$\partial \ell / \partial \theta = (d/\ell)(H_y \sin \theta - H_x \cos \theta)$$

Four-Bar Linkage MA (adapted from Burton [28]).

The moment arm is defined as the partial derivative of the cylinder length with respect to the machine joint angle, which can be related to motion of the four-bar rocker arm CR by way of the angle β ,

$$MA = \partial \ell / \partial \theta = (\partial \ell / \partial \beta)(\partial \beta / \partial \theta)$$

Segment lengths between points are defined as

$$d \equiv \overline{OD} \quad c \equiv \overline{DC} \quad r \equiv \overline{CR} \quad h \equiv \overline{RD} \quad \ell \equiv \overline{HC}$$

where distance h can be computed between its end points R and D ,

$$h = \sqrt{(R_x - d \sin \theta)^2 + (R_y - d \cos \theta)^2}$$

The value of λ can then be computed using the law of cosines, and knowing λ the value of β can be computed from the tangent of line RD ,

$$\cos \lambda = (h^2 + r^2 - c^2)/(2hr)$$

$$\tan(\beta + \lambda) = (R_x - d \sin \theta)/(R_y - d \cos \theta)$$

The cylinder displacement length can then be computed between its attachment points H and C , and differentiated with respect to β ,

$$\ell = \sqrt{(H_x - R_x - r \sin \beta)^2 + (H_y - R_y - r \cos \beta)^2}$$

$$\partial \ell / \partial \beta = (r/\ell)((H_y - R_y) \sin \beta - (H_x - R_x) \cos \beta)$$

Knowing β , the value of γ can be computed from the tangent of line DC ,

$$\tan(\gamma) = (R_x + r \sin \beta - d \sin \theta)/(R_y + r \sin \beta - d \cos \theta)$$

Finally, the rate of change of β with respect to C can be computed by noting that the velocity of points C and D must be equivalent along the direction of line DC ,

$$r \sin(\beta - \gamma) \dot{\beta} = d \sin(\theta - \gamma) \dot{\theta}$$

$$\partial \beta / \partial \theta = d \sin(\theta - \gamma) / r \sin(\beta - \gamma)$$

References

- [1] Ariel, G., 1976, "Variable Resistance vs. Standard Resistance Training," *Scholarastic Coach*, **46**(5), pp. 68–69, 74.
- [2] Axen, K., and Axen, K. V., 2001, *Illustrated Principles of Exercise Physiology*, Prentice-Hall, Upper Saddle River, NJ, Chap. 9.
- [3] Bokelberg, E. H., and Gilmore, B. J., 1990, "Kinematic Design Methodology for Exercise/Rehabilitation Machines Using Springs and Mechanical Advantage to Provide Variable Resistance," 21st Biennial Mechanism Conference, Sept. 16–19, Chicago, IL, ASME, New York, Vol. 24, pp. 279–286.
- [4] Burton, P., 1979, *Kinematics and Dynamics of Planar Machinery*, Prentice-Hall, Englewood Cliffs, NJ, Chap. 1.
- [5] Cabell, L., and Zebas, C. J., 1999, "Resistive Torque Validation of the Nautilus Multi-Biceps Machine," *J. Strength Cond. Res.*, **13**(1), pp. 20–23.
- [6] Dotan, R., and Bar-Or, O., 1983, "Load Optimization for the Wingate Anaerobic Test," *Eur. J. Appl. Physiol.*, **51**, pp. 409–417.
- [7] Elliott, B. C., Wilson, G. J., and Kerr, G. K., 1989, "A Biomechanical Analysis of the Sticking Region in the Bench Press," *Med. Sci. Sports Exercise*, **21**(4), pp. 450–462.
- [8] Evans, W. J., Meredith, C. N., Cannon, J. G., Dinarello, C. A., Frontera, W. R., Hughes, V. A., Jones, B. H., and Knuttgen, H. G., 1985, "Metabolic Changes Following Eccentric Exercise in Trained and Untrained Men," *J. Appl. Physiol.*, **61**, pp. 1864–1868.
- [9] Fleck, S. J., and Kraemer, W. J., 1997, *Designing Resistance Training Programs*, Human Kinetics Publishers, Champaign, IL.
- [10] Friden, J., and Lieber, R. L., 1992, "Structural and Mechanical Basis of Exercise-Induced Muscle Injury," *Med. Sci. Sports Exercise*, **24**(5), pp. 521–530.
- [11] Friden, J., Kjorell, U., and Thornell, L. E., 1984, "Delayed Muscle Soreness and Cytoskeletal Alterations: An Immunocytological Study in Man," *Int. J. Sports Med.*, **5**, pp. 15–18.
- [12] Harman, E., 1983, "Resistive Torque Analysis of Five Nautilus Exercise Machines," *Med. Sci. Sports Exercise*, **7**, pp. 248–261.
- [13] Horowitz, R., Li, P. Y., and Shields, J., 2000, "Control of Self-Optimizing Exercise Machines," *Annu. Rev. Control*, **24**, pp. 201–213.

- [14] Knapik, J. J., Wright, J. E., Mawdsley, R. H., and Braun, J., 1983, "Isometric, Isotonic, and Isokinetic Torque Variations in Four Muscle Groups Through a Range of Joint Motion," *Phys. Ther.*, **63**(6), pp. 938–947.
- [15] Kostic, R., Pesic, M., Pantelic, S., 2003, "The Effects of Resistance Exercises on Muscle Strength in the Recreation of Women," *Phys. Educ.*, **1**(10), pp. 23–32.
- [16] Kraemer, W. J., Mazzetti, S. A., Ratamess, N. A., and Fleck, S. J., 2000, "Specificity of Training Modes," *Isokinetics in Human Performance*, L. E. Brown, ed., Human Kinetics Publishers, Champaign, IL, Chap. 2.
- [17] Kramer, J., and Clarkson, H. M., 1989, "Resistance Torque Patterns of the Nautilus Leg Extension and Leg Curl Machines," *Physiotherapy*, **41**(5), pp. 256–261.
- [18] McCarty, M. F., 1995, "Optimizing Exercise for Fat Loss," *Med. Hypotheses*, **44**, pp. 325–330.
- [19] Montgomery, J. B., and Steadman, J. R., 1985, "Rehabilitation of the Injured Knee," *Clin. Sports Med.*, **4**, pp. 333–343.
- [20] Paulus, D. C., Reiser, R. F., and Troxell, W. O., 2004, "Pneumatic Strength Assessment Device: Design and Isometric Measurement," *Biomed. Sci. Instrum.*, **40**, pp. 277–282.
- [21] Perrin, D. H., 1993, *Isokinetic Exercise and Assessment*, Human Kinetics, Champaign, IL.
- [22] Petrosenko, R. D., Vandervoort, A. A., Chesworth, B. M., Porter, M. M., and Campbell, G. J., 1996, "Development of a Home Angle Exerciser," *Med. Eng. Phys.*, **18**(4), pp. 314–319.
- [23] Pizzimenti, M. A., 1992, "Mechanical Analysis of the Nautilus Leg Curl Machine," *Can. J. Sport Sci.*, **17**, pp. 41–48.
- [24] Signorile, J. F., and Applegate, B., 2000, "Three-Dimensional Mapping," *Isokinetics in Human Performance*, L. E. Brown, ed., Human Kinetics, Champaign, IL, Chap. 6.
- [25] Smith, D. J., 1987, "The Relationship Between Anaerobic Power and Isokinetic Torque Outputs," *Can. J. Sport Sci.*, **12**(1), pp. 3–5.
- [26] Walberg, J. L., 1989, "Aerobic Exercise and Resistance Weight-Training During Weight Reduction," *Sports Med.*, **47**, pp. 343–356.
- [27] Wilmore, J. H., 1982, *Training for Sport and Activity*, 2nd ed., Allyn and Bacon, Boston, MA, Chap. 4.
- [28] Wilmore, J. H., and Costill, D. L., 2004, *Physiology of Sport and Exercise*, 3rd ed., Human Kinetics Publishers, Champaign, IL, Chap. 3.